IAC-22-A6.1.9

On-Orbit SSA: Bespoke and Multi-purpose Optical Sensors to Support In-orbit Servicing

G. Brydon[a]*, T. Harris[b]*, K. Charls[c], E. Hutchinson[c], S. Sara Saji[c], C. McCreath[d]*, L. Blacketer[e]*

[a] *Astroscale UK, Zeus Building, Rutherford Ave, Harwell Science & Innovation Campus, Didcot OX11 0DF, UK* g.brydon@astroscale.com
[b] *Astroscale UK, Zeus Building, Rutherford Ave, Harwell Science & Innovation Campus, Didcot OX11 0DF, UK* t.harris@astroscale.com
[c] *Astroscale UK, Zeus Building, Harwell Science & Innovation Campus, Didcot OX11 0DF*
[d] *Raytheon NORSS, 5A Linnet Court, Cawledge Business Park, Hawfinch Drive, Alnwick, Northumberland, NE66 2GD, UK,* connie.mccreath@norss.co.uk
[e] *Raytheon NORSS, 5A Linnet Court, Cawledge Business Park, Hawfinch Drive, Alnwick, Northumberland, NE66 2GD, UK,* laurence.blacketer@norss.co.uk
* Corresponding Author

Abstract

Astroscale is developing capabilities to address and mitigate the risk associated with space debris through a number of In-orbit servicing (IOS) techniques including Active Debris Removal (ADR), Life Extension (LEX) and End-Of-Life (EOL). These activities rely on space situational awareness (SSA) in order to be conducted safely and effectively, but they themselves also facilitate the use of sensors on orbital platforms to conduct novel *in-space situational awareness* (ISSA) observations. ISSA has potential to enable a range of observations not possible from the ground, with the capability to characterise objects in new ways. This paper provides an overview of Astroscale's work to understand and develop ISSA capabilities. With a number of IOS missions in development, and one in orbit, Astroscale is uniquely placed to apply these to the maturation of ISSA techniques. Astroscale's spaceborne platforms offer the opportunity for a number of optical ISSA observations that ground-based sensors cannot achieve. Spaceborne imagers can observe objects from significantly shorter ranges than ground-based telescopes, allowing detailed characterisation of a range of properties. Favourable observation conditions with no atmospheric interference, indifference to weather, and the potential for observation durations exceeding ground-based best-cases can extend the number and type of objects that can be observed and improve the possible analyses. Some ISSA observations can be conducted with rendezvous proximity operations (RPO) sensors – whose primary purpose is to support RPO and IOS activities – effectively extending the utility of essential hardware. Other ISSA observations require dedicated instruments with abilities such as sensitivity to faint objects, or multispectral imaging. Astroscale is therefore working to understand the ISSA capabilities of a range of different sensor setups, in order to develop capabilities to support and enhance future IOS missions. This paper introduces some key areas of ISSA and describes the activities that Astroscale is conducting to understand and develop relevant techniques. The technical requirements that optical cameras must meet to conduct ISSA is discussed, along with physical limits on observation capabilities. Some ISSA experiments being conducted with the ELSA-d spacecraft are described.

Keywords: SSA, ISSA, IOS, space-based, RPO

Nomenclature

f_r: Bidirectional Reflectance Distribution Function

L_r: surface radiance (power per unit area per unit solid angle)

E_r: surface irradiance (power per unit area)

ρ: surface reflectance (ratio of the total reflected power per unit area to the total incident power per unit area)

I: radiant intensity (power per unit solid angle)

A: bond albedo

F_s: solar flux

σ: object geometric cross-section

α: observation phase angle

ψ: phase function

ψ_{LS}: phase function of a Lambertian sphere

k_d: diffuse reflection coefficient of the Phong model

k_s: specular reflection coefficient of the Phong model

n: specular coefficient of the Phong model (the higher the value, the more closely the specular contribution is confined to the direction of perfectly specular reflection)

β: angle between the reflection direction and the direction of perfect specular reflection

t: observation exposure time

J, J_s, J_{bg}, J_d: electron currents (electrons per unit time) in camera pixel. Subscripts s, bg and d indicate sources of signal, background noise and dark current respectively.

N_r: detector RMS read noise (electrons)

a: camera entrance pupil area

d: camera entrance pupil diameter

Ω: solid angle observed by pixel

L_λ: observed spectral radiance (power per unit area per unit solid angle per unit wavelength)

F_λ: observed spectral flux (power per unit area per unit wavelength)

T_λ: optical transmission of camera at wavelength λ

q_λ: quantum efficiency of detector at wavelength λ

λ: wavelength

θ_d: diffraction-limited angular resolution

Acronyms/Abbreviations

ADR: Active Debris Removal

BRDF: Bidirectional Reflectance Distribution Function

EOL: End-Of-Life

FOV: Field of View

GEO: Geosynchronous Equatorial Orbit

GNC: Guidance Navigation and Control

IOS: In-orbit servicing

ISSA: In-Space Situational Awareness

JAXA: Japan Aerospace Exploration Agency

LEO: Low Earth Orbit

LEX: Life Extension

RPO: Rendezvous and Proximity Operations

RSO: Resident Space Object

SNR: Signal to Noise Ratio

SSA: Space Situational Awareness

UKSA: United Kingdom Space Agency

1 Introduction

In its goal to ensure the sustainable and safe use of space, Astroscale is operating and developing a number of missions to address space debris by reducing its abundance and slowing the rate of new debris generation. To do this, Astroscale is developing a number of in-orbit servicing (IOS) spacecraft.

These spacecraft draw upon and will advance a range of techniques including end-of-life (EOL) services, active debris removal (ADR), and life extension (LEX), each of which plays an important role in space sustainability by taking action at different stages of the spacecraft-to-debris lifecycle. Crucially, these services are underpinned by rendezvous and proximity operations (RPO), whereby Astroscale's servicing spacecraft performs a controlled rendezvous with the client object at very close proximity.

Because of the technical complexity of RPO, as well as the need to ensure safety of two objects in close proximity, RPO requires comprehensive, high fidelity SSA data throughout the mission planning and operation phases in order to understand a range of things about object orbit and state. Some state information requirements, such as rotation characteristics, cannot be fully met by traditional SSA data sources, driving a need for expanded SSA capabilities.

In addition to SSA data, RPO requires detailed information from a range of sensors aboard the servicing spacecraft to perform a number of functions including relative navigation, client pose estimation, and client surface and structure assessment. This generally requires a mix of active (e.g. radar or LIDAR) and passive (e.g. visible and IR cameras) sensors aboard the spacecraft. In their support of RPO, these sensors operate throughout mission phases in which servicer and client are rendezvousing or the servicer is performing manoeuvres or activities at close range to the client. However, there are also mission phases during which these sensors can potentially make observations to support SSA – either because they are not needed for RPO during that phase, or because their RPO function also has SSA utility.

Further to this, an IOS servicer spacecraft can potentially act as a host platform for dedicated ISSA sensors, designed specifically to perform SSA observations. Therefore, RPO platforms simultaneously drive a need for expanded SSA capabilities, and provide an opportunity for conducting novel in-space situational awareness (ISSA) observations (i.e. SSA observations conducted by spaceborne sensors) that can potentially meet that need. Astroscale is therefore conducting work to develop ISSA capabilities, both through characterising the capability of RPO sensors and through the development of ISSA payload concepts.

This paper focusses on the use of optical cameras (both dual-function RPO cameras and bespoke ISSA cameras) for conducting ISSA to supplement traditional SSA sources and support IOS. It provides an overview of Astroscale's ISSA activities, and the missions that are supporting ISSA development (section 2). It then outlines eight ISSA objectives, defined to capture the potential capabilities of ISSA and to guide its development (section 3). This is followed by a discussion of unresolved optical imaging's application to ISSA (section 4). Section 5 touches on the applications of resolved imaging for ISSA. Finally, section 6 provides an overview of imaging experiments being conducted with ELSA-d to understand ISSA capabilities of RPO sensors.

2 ISSA in Astroscale's Missions

Astroscale is developing a number of missions to conduct a variety of IOS activities and to mature technologies and capabilities in this area. Several of these missions are facilitating the development and testing of ISSA techniques, with the aim of understanding how Astroscale can utilise its spacecraft's RPO sensors, as well as deploy dedicated sensors, to conduct routine, operational ISSA with its future missions. This section provides an overview of the missions through which Astroscale is developing ISSA capabilities.

2.1 ELSA-d

End of Life Services by Astroscale - demonstrator (ELSA-d) is a mission to demonstrate a range of debris removal technologies required for future ADR and EOL services. ELSA-d was successfully launched from Baikonur Cosmodrome in March 2021, and has since conducted a number of in-orbit demonstrations (IODs) with its main 175kg spacecraft (servicer) and small 17kg client spacecraft including magnetic capture and relative navigation (see Figure 1). Independently of the mission's servicer-client operations, the servicer's RPO sensor suite – specifically its visible camera (VISCAM) – is now being used to conduct a number of imaging experiments to understand camera ISSA capabilities and the impacts of noise sources (described further in section 6).

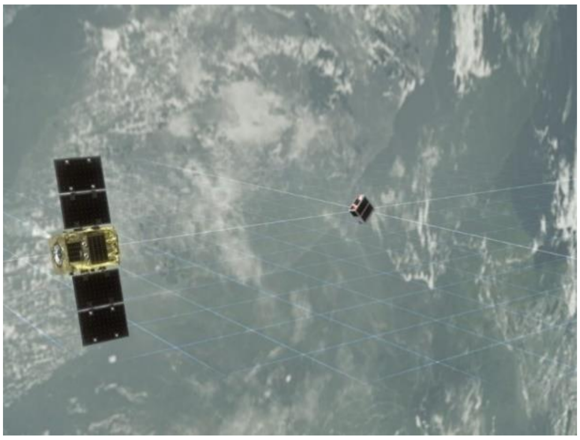

Figure 1: Illustration of ELSA-d servicer and client conducting relative navigation.

2.2 ELSA-M

ELSA-M – the multi-client version of ELSA-d – is an in-development mission which will build on ELSA-d and, with an ability to de-orbit multiple prepared (i.e. fitted with a docking plate and guidance markers) spacecraft with a single servicer, will provide commercial EOL services. As with ELSA-d, RPO will be facilitated by a suite of sensors including cameras. These sensors will provide the opportunity to build on the lessons learned and tools developed from the ELSA-d ISSA experiments that are currently underway.

2.3 ADRAS-J

Active Debris Removal by Astroscale-Japan (ADRAS-J) is an Astroscale mission being conducted as part of the JAXA Commercial Removal of Debris Demonstration (CRD2) project. Its first phase will see ADRAS-J approach and comprehensively inspect a large debris objects using a sensor suite including optical cameras. This mission will provide valuable insight into the utilities of, and operational considerations for, conducting object characterisation through close-range ISSA.

2.4 COSMIC

Astroscale is conducting a UK Space Agency (UKSA) funded study of an ADR mission to de-orbit defunct LEO satellites. The study program, Cleaning Outer Space Mission through Innovative Capture (COSMIC) will further expand on ELSA-M and ELSA-d technology to enable Astroscale to de-orbit defunct, unprepared spacecraft (with no docking or grapple point).

Included in the study is the development of an ISSA payload and operations concept, the purpose of which is to act as a demonstration and test of several novel ISSA observation approaches and analysis techniques, and will be a valuable facilitator of new ISSA capabilities. Both dedicated ISSA hardware and multi-use RPO sensors are being investigated, with the goal of maximising the number of ISSA capabilities that can be developed, tested and matured through the COSMIC mission. Lessons learned from the ongoing ELSA-d imaging experiments will be a valuable input to the COSMIC ISSA development.

3 ISSA Observation Objectives

SSA observations can cover a broad range of information about the orbits and states of resident space objects (RSOs), and are obtained by a variety of techniques. Data obtained through ISSA techniques have the potential to extend the scope of SSA, and introduce new characterisation capabilities. To capture this, we have defined eight ISSA objectives to broadly represent the full range of information that ISSA can in principal provide.

3.1 Objectives I(a) and I(b): Small and Medium Object Detection

These two objectives entail the basic detection of small (herein referring to <1cm, addressed by objective I(a)) and medium (herein referring to 1-10cm, addressed by objective I(b)) objects. A low Earth orbit (LEO) object's size is the primary determiner of whether it can be detected by existing ground-based SSA infrastructure. Many objects within the medium size range and all objects within the small size range are undetectable with current technology, leading to uncertainty about the size, distribution and evolution (including sources and sinks) of their populations.

Medium objects, of which there are an estimated ~1 million [1], make up the population of lethal non-trackable (LNT) objects, which in spite of their difficult-to-detect size can damage, disable or catastrophically fragment spacecraft [2]. To better quantitatively understand and mitigate medium objects' risks to spacecraft, it is necessary to improve detection capability of this size range.

Small objects are even more numerous than medium objects (estimated 330 million objects in the 0.1-1 cm size range[1]), though they generally pose a significantly lower threat to spacecraft. The size, number and lifetime of these objects is such that it will never be feasible to detect the whole population. However, detection of small samples of this population can help to better understand how many objects it comprises, as well as their distribution and evolution. Small object detection is not directly relevant to spacecraft operations, but has a wider academic importance given the links between debris objects of all sizes [3].

3.2 Objective II: Cataloguing Large Objects

The large (herein >10cm) object population includes all operational and previously-operational spacecraft, as well as other sizeable debris, and includes approximately 35-40,000 objects. Approximately 22,000 of these objects are tracked via a number of global ground-based sensor systems [1]. The knowledge of large objects' locations and velocities, and the ability to perform orbit determination (OD) is essential to SSA services, and is what most current systems are set up to provide. ISSA Objective II entails collecting this information from spaceborne sensors – either entirely independently, or as a supplement to ground-based observations (e.g. ISSA observations may feed into OD alongside ground-based data to improve fidelity).

3.3 Objective III: Targeted Tracking

Targeted tracking entails the observation of a single, specific object in order to determine its position and orbital elements to a higher fidelity than is achieved through the standard cataloguing process, or to maintain object custody. Increase in fidelity may be in terms of positional accuracy, but could equally be the temporal accuracy or coverage of the measurements. This targeted tracking may be required during higher-risk operations such as RPO, or in the event that an operator's spacecraft exhibits unexpected behaviour.

As with objective II, capabilities to perform this tracking already exist within ground-based infrastructure. Studying the scope for space-based sensors to address this objective is motivated by the potential to achieve improved measurement accuracy and/or greater coverage.

3.4 Objective IV: Unresolved Targeted Characterisation

Characterisation entails the measurement of any aspects of an object's state other than its position and orbital motion. A primary example of this is the determination of an object's attitude and rotation (i.e. tumble rate), but it can also entail the assessment of object damage, subsystem ageing/health, and fault diagnosis, amongst other things.

This objective deals specifically with characterisation observations in which the object is not spatially resolved. This commonly takes the form of photometric analysis, extracted from image streaks [4], [5].

3.5 Objective V: Flyby Resolved Imaging

We define flyby observation as an observation conducted during a conjunction of the observing spacecraft and observed object, without any prior modification made to the observer's orbit. It is essentially an opportunistic observation, conducted when the observer and object happen to be in a suitable geometry.

Flyby resolved imaging is therefore the collection of resolved images of an object during a flyby of sufficient imaging conditions (a resolved image is technically one in which the observed object spans at least three pixels, though significantly higher resolutions than this are desirable).

Flyby observation typically leads to large imaging distances (e.g. several tens of kilometres) and high relative speeds.

3.6 Objective VI: Stand-off Resolved Imaging

If resolved imaging is instead conducted from a platform whose orbit has been modified in order to minimise relative observer-object velocity, we define that as stand-off imaging. Stand-off imaging provides longer imaging opportunities than flyby imaging, and allows a more favourable imaging geometry to be arranged. Stand-off imaging can be conducted over a range of distances, from kilometres down to hundreds of metres, allowing a higher spatial resolution than flyby imaging. Achieving stand-off imaging requires manoeuvring in order to match orbits, but does not require a full rendezvous with the object, with which there is a greater risk and cost associated.

The stable and prolonged observation opportunities provided by stand-off imaging allow good spatial resolution, capable of determining object geometry and orientation, and the deployment state of structures such as solar arrays and booms. Image sequences captured over a long enough duration can facilitate the measurement of rotation rate and axis, along with the time evolution of other characteristics of the object.

3.7 Objective VII: Short-range Resolved Imaging

Short-range resolved imaging is conducted at metre distances, when the observer and object have safely rendezvoused. Achieving this imaging scenario requires significantly larger effort than either flyby or stand-off imaging, and it would generally be expected that short-range imaging would be conducted on specific objects that were identified and designed-for prior to mission launch. Because of the distances at which it is conducted, short-range resolved imaging allows the greatest level of resolution and detail of any mode of observation. It can facilitate the assessment of surface and structure condition (including ageing and damage), pose estimation, and 3D mapping.

4 ISSA With Unresolved Imaging

Addressing all eight of the ISSA objectives outlined above requires a range of techniques and hardware. Through its ISSA development work – facilitated by the missions described in section 2 – Astroscale is investigating the requirements and capability to address all of the objectives. However, addressing all eight of the objectives in a single paper is not possible. This paper therefore focusses on optical unresolved imaging (relevant to objectives I-IV), discussing some important considerations for its application to ISSA, particularly for objectives I and IV.

4.1 Radiometric Modelling of ISSA

The performance of an optical camera when observing space debris or spacecraft is largely dependent on its sensitivity and the object's brightness. Development of optical ISSA observation techniques must therefore be informed by sound radiometric modelling of both the observed object and the ISSA instrument.

4.1.1 Space Debris and Spacecraft

When conducting ISSA with an optical camera in the visible and near-visible wavelengths, an object (spacecraft or space debris) is seen due to its reflection of sunlight toward the observing instrument. The ratio of a surface's reflected radiance L_r (in a given direction) to the incident irradiance E_i of the surface (from a given direction) is defined as the surface's bidirectional reflectance distribution function (BRDF) f_r.

$$f_r = \frac{L_r}{E_i} \quad (1)$$

In the most general case it is a function of the direction of incidence, the direction of reflection, and the surface material at the point of reflection. In the simplified case of a Lambertian (purely diffusely reflecting) surface, the BRDF is given by

$$f_r = \frac{\rho}{\pi} \quad (2)$$

where ρ is the reflectance (ratio of the total reflected power per unit area to the total incident power per unit area). A common (albeit very simplified) model for space debris or spacecraft when considering their optical signature is that of a sphere with a uniform Lambertian surface. The radiant intensity I (power per unit solid angle) reflected toward an observer by a Lambertian sphere is given by

$$I(\alpha) = \frac{2}{3\pi} A\, \sigma\, F_s\, \psi(\alpha) \quad (3)$$

where the bond albedo A is equal to the Lambertian surface's reflectance and commonly taken to be 0.175 in literature [6]. The phase function of a Lambertian sphere is given by

$$\psi_{LS} = \frac{(\pi - \alpha)\cos\alpha + \sin\alpha}{\pi} \quad (4)$$

The only dependence that object brightness has on observation geometry when dealing with a Lambertian sphere is the dependence on phase angle. This simplifies brightness estimations of objects, but removes dependence on object attitude, geometry and surface material distribution that can be important when considering certain observations such as photometric characterisation. Spacecraft can generally be more accurately represented by cuboids and/or planar surfaces, whilst accurate representation of their surface reflections can require the inclusion of both diffuse (Lambertian) and specular components. The Phong surface model accounts for both diffuse and specular reflections, and its BRDF is given by

$$f_r = k_d \frac{1}{\pi} + k_s \frac{n+2}{2\pi} \cos^n \beta \quad (5)$$

4.1.2 Optical Cameras

The signal to noise ratio (SNR) for a measurement captured by an optical camera's pixel is given by

$$SNR = \frac{J_s t}{\sqrt{J_s t + J_{bg} t + J_d t + {N_r}^2}} \quad (6)$$

The pixel electron current J caused by fluxes and/or radiances is given by

$$J = \int a\, T_\lambda (\Omega L_\lambda + F_\lambda) q_\lambda \frac{\lambda}{hc}\, d\lambda \quad (7)$$

where the integral with respect to wavelength is performed over the instrument's range of spectral sensitivity.

4.2 Object Detectability

For space-based sensors – just as with ground-based sensors – object flux is a major determiner of whether an RSO can be detected by an unresolved observation. A major benefit of using space-based sensors is therefore the ability to get closer to the observed objects (in addition to bypassing the atmosphere) – meaning that objects have greater apparent brightness.

However, the use of a space-based sensor limits cameras to smaller aperture sizes than can be deployed in ground-based observatories, having the opposite effect of reducing the achievable sensitivity. Figure 2 plots object brightnesses (assuming Lambertian spheres of bond albedo 0.175, observed at a phase angle 90°), along with indicative values for an optical camera's minimum detectable flux (taken to be the flux for which SNR=4). The following camera parameters are used:

- Ω: 0.27 μ sr
- T: 0.8 (spectrally constant)
- q: 0.55 (spectrally constant)
- Sky background radiance: $2.6\text{x}10^{-9}$ W m^{-2} sr^{-1} (spectrally constant)
- J_d: 10 e^{-} s^{-1}
- N_r: 15 e^{-}
- Spectral range: 450-700 nm

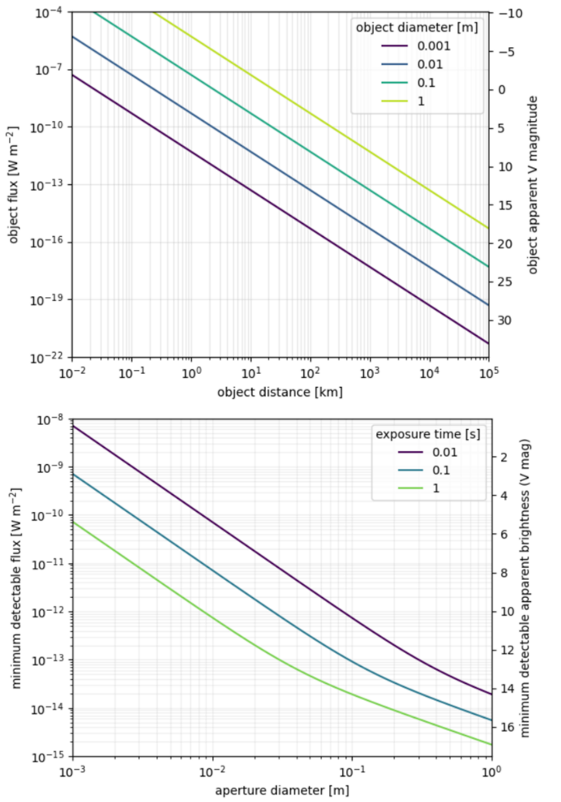

Figure 2: Top – Reflected flux from an object (Lambertian sphere with A=0.175) as function of object distance and diameter, when observed at phase angle 90°. Bottom – Approximate minimum detectable flux (SNR=4) for an example optical camera as a function of its aperture diameter and exposure time (assuming the object position in FOV remains fixed). Camera parameters are listed in main text.

To estimate how this key link between aperture size and object detectability impacts a space-based camera's ability to detect sub-10cm objects (ISSA objective I), a simulation was conducted using ESA's Program for Radar and Optical Observation Forecasting (PROOF) tool [7]. This tool produces statistics for camera FOV crossings for debris objects ranging in size from 1mm upwards. Combining crossing statistics with the radiometric modelling of section 4.1, we estimated the number of 'detectable' (the object would be imaged with SNR ≥4 if imaging was taking place at time of FOV crossing) crossings of 1-10cm objects within a 24 hour period for a camera in polar orbit with 5x5° FOV and boresight perpendicular to both the orbital plane and Sun-Earth line. The results are plotted in Figure 3.

It demonstrates that aperture diameter has a significant impact on the ability for ISSA to extend and improve 1-10cm object detection capabilities. For apertures on the order of a cm, only a handful of detectable objects may cross in any given day, and this would be too few to have statistical value (this effectively rules out the use of RPO cameras for ISSA objective I). Use of a larger bespoke ISSA camera with ~10cm aperture is feasible, and could potentially allow ~100 detections per day – likely sufficiently high to provide some valuable statistical information on the distribution and evolution of the sub-10cm debris population. It is however worth noting that conducting observations in a way that captures all of the detectable crossings is a significant technical challenge of its own (requiring the continued and frequent capture of many images and the handling of large volumes of data), but this issue is beyond the scope of this paper. Metre-scale apertures are capable of thousands of detections daily, but are too large and massive to feasibly be used as an ISSA instrument. Through modelling and in-orbit tests (such as those being conducted with ELSA-d (section 6), and those planned for COSMIC), research into the practicalities of <10cm object detection through optical imaging is ongoing.

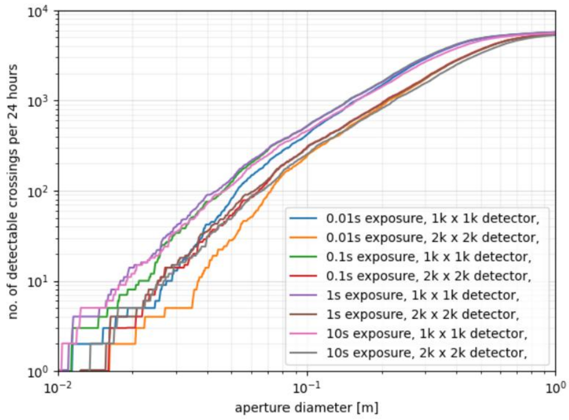

Figure 3: Number of detectable (object would be imaged with SNR≥4) 1-10cm objects crossing camera FOV in 24 hour period as function of camera aperture, resolution and exposure time. Camera parameters are FOV=5x5° T=0.8, q=0.55, J_d=10 e^- s^{-1}, N_r=15 e^-, bandpass=450-700nm. Camera is in a polar orbit with boresight perpendicular to both orbital plane and Sun-Earth line.

4.3 Photometry

Unresolved photometry of RSOs is an effective way of understanding an object's state based on its brightness and brightness variation. A common and important application of photometry is attitude and attitude rate assessment for spacecraft and large debris objects [8]–[10]. This is an application of high importance to Astroscale's future services due to the need to understand the spin state of a client object before conducting proximity operations or docking. Through its COSMIC mission study, Astroscale is working with Raytheon NORSS to develop ISSA techniques that can increase the reliability and capability of photometric attitude assessment.

4.3.1 Long-duration Photometry

Passive optical photometry is a valuable technique for estimating RSO spin state, including that of LEO spacecraft and large debris [8]–[10]. This is demonstrated by the Russian Mini-Mega-TORTORA (MMT) wide-field monitoring system and its associated database. The MMT collects light curves of a wide variety of spacecraft and debris objects, the majority of which are stored in a publicly accessible online database [11]. This database allows raw light curve data to be viewed, along with derived products such as normalised light curves and assessments of whether an object is aperiodic (not spinning) or periodic (in which case an estimated spin period is also provided).

A shortfall in the data available from MMT and other ground-based light curve observers is typical light curve duration, and the associated limit to characterisable spin period. Safely conducting ADR and EOL requires detailed understanding of the object's spin state – including the angular rate, the axis of rotation and the evolution of each of these – and necessitates the characterisation of a wide variety of spin states. Achieving this requires the ability to capture light curves spanning as long a duration as possible – something which is inherently limited for ground-based observatories.

Whilst the possible durations of ground-based light curves of LEO objects vary greatly, they are inherently limited by the observer's local horizon, and on an observation-to-observation basis are impacted by weather effects. Ground-based light curves therefore have typical durations on the order of ~100s. This limits the level to which spin state can be characterised, and whilst favourable viewing conditions and observation geometries can allow ground-based observations of longer durations (~1000s), this is object and observatory dependent and cannot be relied upon for all objects. There is therefore a gap between the current capability to characterise object spin rates, and the required capability for supporting IOS missions, and closing this gap through ISSA is an area of key importance.

For a space-based observer, clear line-of-sight of an observed object can persist for significantly longer than for a ground-based sensor. ISSA systems do indeed therefore provide the potential to close this gap by conducting long-duration photometry, which we define to be a single photometric dataset (though it can comprise multiple individual observations) spanning ≥1000s.

As an example, Figure 4 plots the duration of uninterrupted visibility (satisfied as long as there is a clear LOS between object and observer) between a LEO observer and LEO object in coplanar, circular orbits (the optimum geometry for maximising uninterrupted observation duration). The observed object is in a 750km altitude orbit.

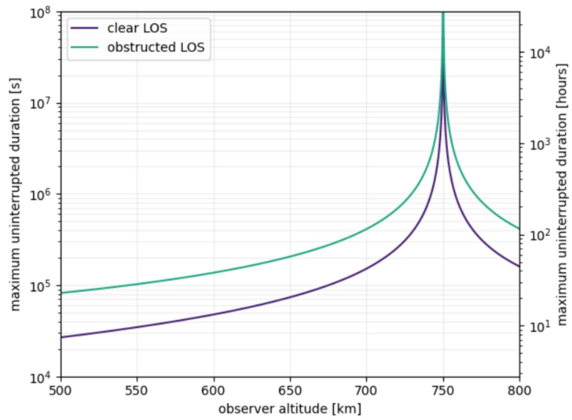

Figure 4: Duration for which observed LEO object in 750km circular orbit is continuously connected to observer by a clear LOS (not intersecting the Earth or the atmosphere below 100km altitude). Observer and object are in co-planar circular orbits.

Figure 4 demonstrates that a space-based sensor can, under optimal observational conditions, maintain a clear view of an object for durations on the order of 10^4 and even 10^5 seconds – significantly longer than a ground based observer. However, line of sight visibility of an object does not guarantee that it can be observed. Particularly for photometry observations, a good quality signal is required to make accurate measurements of an object's brightness. In addition to maintaining a clear LOS, it's therefore also necessary to keep the Sun and Earth out of and away from the FOV during observation to minimise background noise, sensor saturation, and stray light effects. Equally, it's necessary for the observed object to remain illuminated for the full observation duration.

To account for these requirements and perform a more realistic assessment of possible space-based observation windows, a simulation was conducted by Raytheon NORSS using their Brightness Analysis, Lightcurve Determination and Reproduction (BALDR) tool. The simulation considered an object in a LEO orbit typical of many spacecraft and debris objects. The details of the object's orbit are listed in Table 1.

Table 1: Orbital parameters of observed object at BALDR simulation start epoch (2021/09/01).

Parameter	Value
Inclination	99°
Right ascension of ascending node (RAAN)	200°
Perigee	780 km
Apogee	796 km
Argument of perigee	50°

For an observer in a circular orbit, the simulation modelled 6 months of orbits to identify the periods for which the object was visible to the observer. This simulation was repeated for 9 different observer altitudes (with all other aspects of the observer orbit matching those of the observed object at simulation beginning). In addition to satisfying clear LOS between the two objects, periods of visibility also satisfied:

- Sun and Earth were outside the 50x50° FOV
- The object was illuminated by the Sun
- The phase angle of the observation was ≤100°

The mean observation window duration and the number of individual observation windows over a 6 month period are plotted in Figure 5.

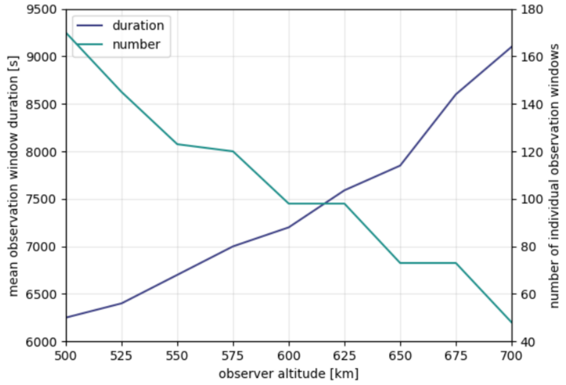

Figure 5: Average duration of observation window and number of observation windows over 6 month period as function of observer altitude (circular orbit). Orbit parameters of observed object at beginning of simulation period are listed in Table 1.

With these additional observational constraints, the possible observation durations do decrease, but still remain on the order of 5000-10,000 s – significantly longer than is possible from ground. These extended observation windows can improve the ability to detect periodic variation in an object's brightness, increase confidence in spin rate measurement, and better enable the identification of the object's spin axis orientation.

It is worth noting that whilst long-duration photometry is necessary to enable accurate spin rate assessment of a wide variety of objects, it brings additional challenges. The larger the time period that a light curve spans, the more the observation geometry changes over the duration of the light curve. For a space-based long-duration light curve, phase angle and range of observation can both change significantly, and with the object potentially moving several tens of degrees in the sky as seen by the observer, it can be necessary to slew the observing spacecraft during light curve collection.

Whilst changes in observation range can be easily corrected for, phase angle effects depend on object geometry and surface materials, and separating their contribution to brightness variation from the contribution of object rotation can potentially be less straight forward. Slewing during an observation would add the additional complexity of non-constant noise conditions (e.g. from background and stray light). Through the COSMIC mission study, Astroscale and Raytheon NORSS will continue to investigate the practicalities of and requirements for conducting long-duration photometry through ISSA observations, with the end goal of conducting in-orbit demonstrations and maturations of the technology.

4.3.2 Photometric Sensitivity

Measuring an object's light curve requires a greater radiometric fidelity than object detection and astrometry observations (ISSA objectives I-III). To characterise temporal variations in an object's brightness a higher SNR is necessary than required for simply identifying the presence of an object's streak within an image (see also section 6.2).

A tumbling object's brightness can vary significantly depending on its spin axis, geometry and surface materials. This can make it difficult to predict how bright an object will be during observation, and therefore how sensitive an instrument needs to be to conduct useful photometry.

However, modelling of an object's reflectance can be used to constrain expected brightness ranges and define instrument requirements and observation limits.

To demonstrate this, we here model a simple spacecraft as a single cube of dimension 0.5x0.5x0.5m. The cube has four solar array-like faces (faces intersecting the x and y axes of the craft) and two aluminium-like faces (faces intersecting the z axis), whose reflections are described by the Phong model (section 4.1.1). The 'solar array-like' faces exhibit a significant specular reflection, with Phong parameters kd=0.4, ks=0. 2 and n=10. The 'aluminium-like' faces represent a more diffusely-reflecting, duller surface with Phong parameters kd=0.08, ks=0. 02 and n=10.

A Monte Carlo simulation was used to model the possible brightness of the object under different observation conditions when illuminated by solar radiation at 1 AU. Specifically, the reflected brightness is simulated at observation phase angles from 1-180° at 1° intervals. At each phase angle, 10,000 brightnesses are calculated, each with the spacecraft's yaw, roll and pitch randomised. The resulting brightnesses are plotted in Figure 6.

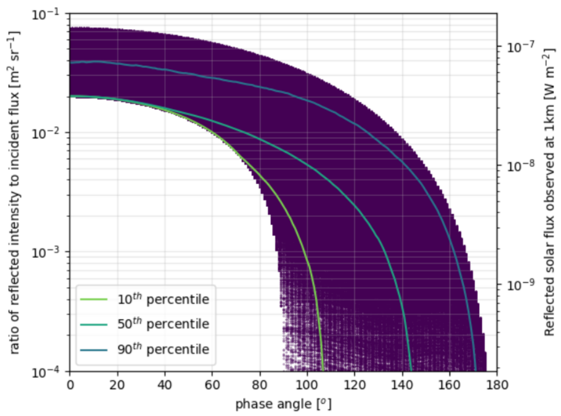

Figure 6: Simulated brightnesses of a cube (spacecraft) at observation phase angles 0-180° (in 1° increments). Four of the cube's faces are solar arrays, whilst the other two are aluminium as described in the main text. 10,000 random orientations of the spacecraft are simulated at each observation phase angle. The 10th, 50th and 90th percentiles of cube brightness are indicated.

Figure 6 demonstrates how significant an impact the orientation of a spacecraft can have on its observed brightness. At large phase angles (>90°) the 10th and 90th percentiles of spacecraft brightness differ by >2-3 orders of magnitude, and due to self-shadowing at certain orientations, some spacecraft attitudes result in no light being reflected toward the observer. At smaller phase angles (≤80°) the spacecraft's brightness is less variable (~1 order of magnitude between brightest and faintest), and is always non-zero, therefore making it more conducive to reliably obtaining photometric observations.

If space-based photometry is to be used operationally to support a mission – for example by characterising the spin rate of an ADR client prior to rendezvous – it is necessary to use simulated data to determine any constraints required on observation geometry (e.g. maximum phase angle) and instrument performance. For example, taking a maximum observation phase angle of 80° from Figure 6 (selected because it is approximately the largest phase angle for which minimum and maximum brightnesses are within one order of magnitude of each other), the 10th percentile value for the ratio of reflected intensity to incident flux is 4×10^{-3} m^2 sr^{-1}. This corresponds to a reflected intensity of 0.0075 W sr^{-1} when the object is under solar illumination at 1AU. Figure 7 plots the maximum distance from which this intensity can be measured with an SNR ≥4 as a function of camera entrance pupil diameter. Image exposure time and object dwell time (the time for which the observed object remains over a single pixel) are 5s and 0.1s respectively. All other parameters are the same as listed in section 4.2.

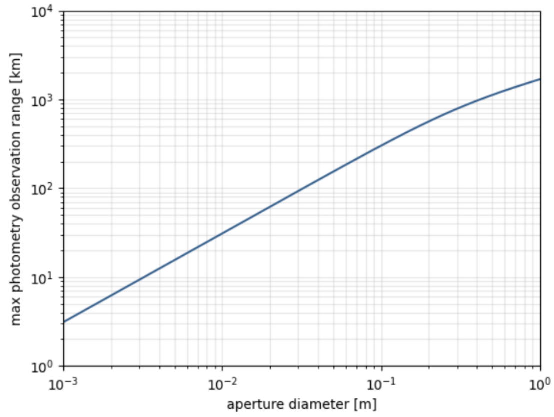

Figure 7: The maximum distance at which photometry of the cuboid spacecraft modelled in Figure 6 can be conducted with SNR ≥4 as a function of camera aperture diameter. Image exposure time is 5s and object dwell time is 0.1s. All other parameters are the same as listed in section 4.2.

Figure 7 indicates that photometric ISSA observations are potentially feasible for a range of camera sizes, and need not be restricted to large-aperture instruments. Whilst photometry at ranges in excess of 1000km requires apertures on the order of several tens of cm (meaning high volume, high mass cameras), smaller cameras (apertures on the order of a few cm) may be capable of obtaining light curves at distances in the low hundreds of km – making LEO-LEO photometry feasible. Conjunctions of this distance and less between LEO objects are common, especially if the observing spacecraft is purposefully placed in an orbit close to objects of interest.

Additionally, for an IOS mission – which has to close to very short range of its client – 10-100km range photometry can be conducted well in advance of rendezvous, allowing early characterisation of spin state to feed into mission planning and operation.

Because short-range RPO cameras require small (a few mm) apertures to achieve focus at short distances, their application to unresolved photometry is limited.

Through ongoing work on modelling and ultimately testing of space-based photometry, Astroscale is working to identify the necessary observational hardware for conducting photometric ISSA with its future platforms, and its compatibility with other ISSA and RPO sensor functions.

5 ISSA with Resolved Imaging

Resolved imaging is the spatially resolved observation of an object of interest – in the case of this paper, using a camera. For an object to be resolved, its size as seen by the observer must exceed the observing instrument's minimum resolvable angle. Achieving resolved imaging therefore imposes a geometric constraint on the observer-object geometry.

Resolved imaging provides spatial information, allowing the assessment of object attitude, object structure, the condition of surfaces, and the deployment status of mechanisms – along with the evolution of all of these. As with tumble rate assessment, these are key aspects that must be understood about an object before it can be serviced, and resolved imaging is therefore an important potential facilitator of future IOS missions.

The resolution of an imaging system can be affected by all aspects of its design, and each of its components. However, all imagers are subject to a fundamental physical resolution limit – known as the diffraction limit – imposed by their aperture size (specifically, due to the diffraction of the light as it passes through the aperture). A camera for which aperture diffraction is the resolution's limiting factor is known as diffraction-limited. The resolution of a diffraction-limited camera is approximated by the Rayleigh criterion, which gives the smallest possible resolvable angle θ_d as

$$\theta_d = \sin^{-1}\left(1.22\,\frac{\lambda}{d}\right) \quad (8)$$

The spatial diffraction-limited resolution of a camera is plotted in Figure 8 as a function of imaging distance and aperture diameter.

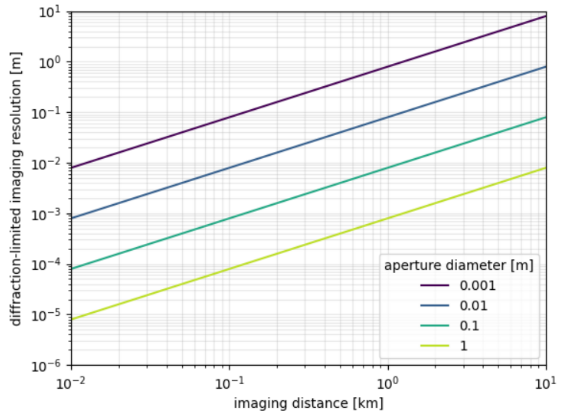

Figure 8: Diffraction-limited resolution of a camera as a function of imaging distance and camera entrance pupil diameter.

If instrumental components other than a camera's aperture are the limiting factor for resolution, then the camera is described as instrument-limited. Generally, the most important factors in whether a camera is instrument-limited are the number of pixels on its detector and the geometry of its optics. For a given detector, image resolution degrades as FOV size increases, whilst for a given FOV, image resolution increases as the number of pixels in the detector increases. Figure 9 plots the spatial resolution of an instrument-limited camera as a function of imaging distance and FOV width. The camera has a square FOV and a 2000x2000 pixel detector.

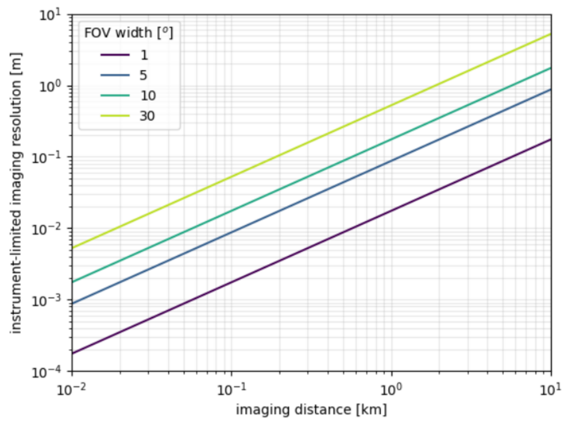

Figure 9: Instrument-limited resolution of a camera with square FOV and 2000x2000 pixel detector, as function of imaging distance and FOV width.

Resolved imaging allows detailed object characterisation, including attitude assessment and surface assessment. The higher the resolution of the imagery, the more detailed the characterisation can be, but even at low resolutions valuable insight can be gained. This means that resolved imaging doesn't necessarily have to be confined to large, high-performance cameras or short-range observations, and a variety of hardware – including RPO sensors – can potentially perform this function.

As an example, Figure 10 shows two sets of simulated image sequences of a fictitious spacecraft (approximately 1m long, three solar arrays mounted on gold MLI-covered bus). The top image set of the figure demonstrates the differences in spacecraft appearance when viewed at different resolutions. Even at poor resolutions (40-100cm) information about spacecraft shape and orientation exceeding what is available from ground-based SSA is available. At the higher resolutions, significant detail and pose information is obtained.

For small RPO cameras (e.g. ~mm apertures, wide FOVs), achieving resolutions <100cm requires approaching the object to within at least ~1km (at which distance RPO sensors may already be characterising the object for their own functions, and by which time it is already preferable to have a good understanding of the object's state). By using larger (e.g. apertures of a few cm diameter), higher-resolution cameras (either bespoke ISSA cameras or RPO cameras augmented to increase their resolution), resolutions of 10s of cm can be achieved from multiple km, whilst cm resolutions can be achieved from ~1km. This allows characterisation or pose estimation of an object *in advance* of performing rendezvous (or potentially even orbit matching), allowing it to inform subsequent operations or inform an abort (preventing wasted resource use for unnecessary rendezvous).

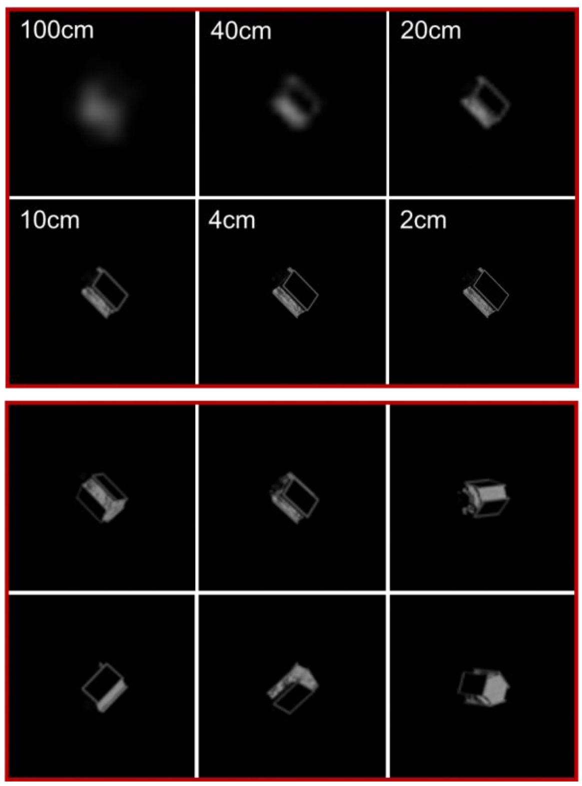

Figure 10: Simulated ISSA resolved imagery. Top: A simulated approach image sequence demonstrating the effect of increasing resolution. Bottom: A simulated attitude observation sequence demonstrating attitude evolution imaged at a resolution of 10cm.

6 ELSA-d ISSA Experiments

Since its launch in 2021, ELSA-d (section 2.1) has conducted several in-orbit demonstrations of RPO and EOL techniques, including magnetic capture and relative navigation between its main spacecraft (servicer) and smaller client spacecraft [12]. To perform these operations, the servicer is equipped with a sensor suite that includes several optical imagers. Separately to the mission's in-orbit demonstrations, one of these imagers – the visible camera (VISCAM) – is currently being used to perform ISSA observations of LEO and GEO objects. These experiments are currently ongoing, with significant analysis still to be completed. This section therefore provides a brief overview of the experiments.

The main purpose of these imaging experiments is to understand the key processes and challenges involved in ISSA observation. Equally, they are being used to characterise the camera's ISSA capabilities bearing in mind that it was designed solely for RPO-related observations. Understanding the capabilities and capability gaps of the VISCAM and similar RPO cameras will be an important input to the development and exploitation of ISSA systems on future Astroscale missions. The experiments entail a variety of observations including opportunistic imaging of LEO objects (imaging objects that pass relatively close when they are in a favourable position), attempts to image GEO objects, and imaging of stars.

6.1 Imaging Windows

In contrast to a ground-based sensor, a space-based sensor has a greater number of degrees of freedom and a different set of constraints for when and under what conditions an object can be observed. A number of key considerations for identifying observation windows are listed below:

- Line of sight: observation windows only exist for times when the observer and imaged object are connected by an unobstructed LOS. Due to its altitude, a LEO-based observer has a greater area of sky over which it can achieve LOS of objects (e.g. for an observer at 650km altitude, the Earth and its atmosphere blocks ≈30% of the total sky, compared to >50% for ground-based observers). Selecting observation windows by this criterion alone results in a large number of candidates.
- Illumination conditions: unlike ground-based observations, it is not necessary for the observer to be in local night time. It is however necessary for the imaged object to be illuminated at an observation phase angle that is sufficiently small to ensure the Sun is kept out of the FOV, and the object exhibits a strong reflection. For the ELSA-d imaging experiments a maximum phase angle of ~90° is generally imposed. This significantly cuts down the number of viable observation windows.
- Stray light and detector saturation: imposing a maximum phase angle (as per previous point) is sufficient to prevent saturation of the detector by the sun or its stray light. However, Earth's reflected light is also significant, and it is therefore necessary to ensure that none of the Earth's illuminated disk impinges on the FOV, and that the entirety of the illuminated Earth is sufficiently far from the FOV to minimise stray light. This constrains suitable imaging LOSs but can also constrain spacecraft attitude, and further restricts the number and length of possible observation windows.
- Observer attitude: additional non-imaging constraints on spacecraft attitude must be satisfied, such as ensuring star trackers are not blinded, and this can further reduce the number of possible observation windows.
- Range: LEO-to-LEO observations can be conducted at significantly shorter ranges (e.g. ~100km) than possible from the ground if the observer and observed object orbits allow it. Equally, observations can also occur from larger distances (e.g. ~1000km). Depending on the need for high signal, observation range can be used to prioritise certain observation windows.
- Relative angular velocity: the relative angular velocity of a LEO observer and LEO object can vary significantly depending on the two objects' orbits. As with range, angular velocity can be used as an observation window selection criterion. If high signal is desired, a low angular velocity may be needed (to increase dwell time), whilst high-fidelity astrometry might necessitate a long streak and therefore a larger angular velocity.

6.2 Imaging Experiments Overview

Thus far, the ELSA-d imaging experiments have comprised attempts to image a variety of objects with a range of observational configurations and varying levels of success. Some example images from the experiments are presented discussed in this section.

Noise sources are a major factor in ISSA imagery and can impact whether an observation is useable. This is a significant factor for ELSA-d's VISCAM, as it was designed to perform metre-range resolved imaging of a well-illuminated client spacecraft, and not ISSA observations of faint point sources.

A number of noise sources exist within the camera that posed minimal issue for its nominal operations, but that significantly limit ISSA functionality. Hot pixels (pixels which accumulate charge at a high rate and in the absence of any signal) are relatively abundant in the VISCAM (having been on orbit and exposed to radiation for 18 months).

At first glance hot pixels can be mistaken for stars (see Figure 11), but are distinguishable by their high level of sharpness (each one being confined to a single pixel) and fixed position between images. Hot pixels can be removed from image sequences through averaging and subtraction, whilst more rigorous handling requires the collection of dark frames (accompanied by detector temperature data) to characterise hot pixel charge leakage rates and dark current rates.

Hot pixels can also be partially removed through 'annealing' – heating the camera's detector to a temperature of ~30°C [13]. This can be achieved through a dedicated heater, or if the camera's temperature is regulated by a radiator, by exposing the radiator to solar illumination. This is not an option for ELSA-d's VISCAM (and was entirely unnecessary for RPO function), but for a dedicated ISSA payload, hot pixel annealing may be an important design and operation consideration.

Figure 11: An un-processed ELSA-d VISCAM exposure displaying numerous hot pixels. At first glance they look like stars, but are recognisable from their sharpness and constant position throughout image sequences.

Also significant is stray light, which comes from bright sources (i.e. the Sun and Earth) near to or inside the FOV and makes its way to the detector via unwanted reflections and scattering within the camera's optics. It reduces image contrast and can overpower the faint signals of the intended ISSA targets. It's important to note that stray light can come from objects outside of the FOV, and the extended and bright surface of the Earth is therefore a major stray light source for LEO ISSA observations. For some ELSA-d imaging attempts, the Earth's stray light has been found to be strong enough to saturate the detector when employing exposure times of several seconds. When straylight is less significant, efforts can be made to remove it. For images captured on a short timescale under the same observation geometry, stray light remains relatively constant across images. This allows the mitigation of stray light through image averaging and subtraction (taking the average of the full image set and subtracting it from each individual image). More thorough handling would require pre- and in-flight characterisation of the camera's stray light behaviour. Ideally, any ISSA camera would also mitigate straylight through its hardware design, by the inclusion of a baffle, and by its positioning away from reflective protruding objects on the spacecraft. Figure 12 shows an example of stray light within an ELSA-d image.

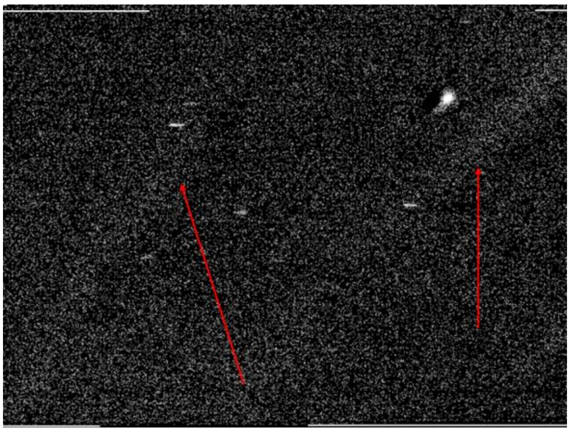

Figure 12: A VISCAM image with stretched contrast and brightness to highlight two diffuse stray light features (indicated by red arrows).

Figure 13 shows a representation of the same data as Figure 12, this time processed to remove stray light and background noise. The image is one of a sequence of 5s test exposures, not intended to capture any object in particular. Six stars are indicated by red arrows, appearing as short streaks due to a constant slew of the spacecraft during imaging. The directions of the arrows indicate the directions of the associated stars' motion. Streak length and direction is an effective way to verify objects as stars and distinguish them from other noise sources, and in this vein it can be beneficial to capture ISSA observations whilst purposefully performing a slow and constant slew of the spacecraft.

The blue arrow indicates a bright blob whose motion direction was opposite to the stars. Whilst its high brightness suggests it could be a nearby (i.e. LEO) object, its low angular speed makes this unlikely (c.f. the object streak length of Figure 14). Its source is currently unconfirmed but assumed to be an internal reflection (stray light) feature from the Sun, which was only a few degrees away from the camera's FOV at time of imaging.

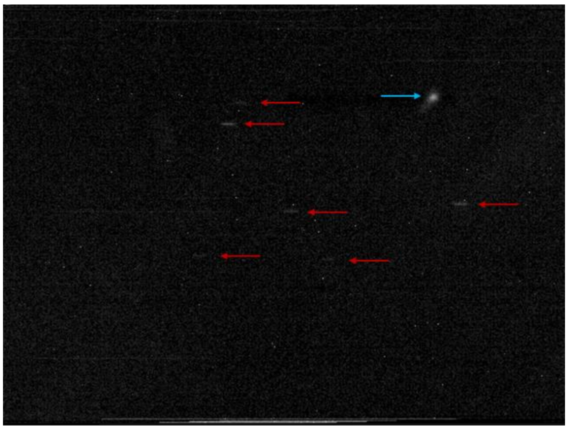

Figure 13: One image of a sequence of 5s exposures captured whilst pointing the camera toward 'empty' space (i.e. not aimed toward a specific object). The image was captured during a steady slew of the spacecraft, and has been processed to remove background noise. 6 stars (red arrows) and one unidentified signature (blue arrow) can be seen. The

arrows indicate the direction that their feature was moving across the FOV.

Figure 14 is an image from a LEO object imaging sequence, processed to remove background noise. The object is seen as a streak in the top half of the image (indicated by blue marker). Four stars can also be seen (red arrows) as short streaks due to minor spacecraft rotation. Note that the object streak is only marginally brighter than the image's noise floor (and has an SNR of approximately 2), and significantly fainter than the stars. The streak's geometry is well defined, making it suitable for astrometric measurements, but the low SNR would make it unsuitable for any photometric characterisation (see section 4.3). Streak brightness versus background noise is an important consideration when planning observation exposure time, as well as when identifying suitable observation windows (e.g. shorter-range observations can be prioritised if high brightness is desired).

Uncertainty in exact image capture time, along with uncertainty in a target object's propagated orbit, can lead to uncertainty in the exact position within the FOV an object will be captured. Streak length and orientation are less affected by these uncertainties, and are therefore more reliable metrics by which to confirm whether a captured streak is the intended object. Use of stars within the images is essential for precisely constraining an image's astrometry, and in combination with a model of the camera's geometric distortions, can facilitate very accurate astrometry of objects within images (e.g. as required for ISSA objectives II and III).

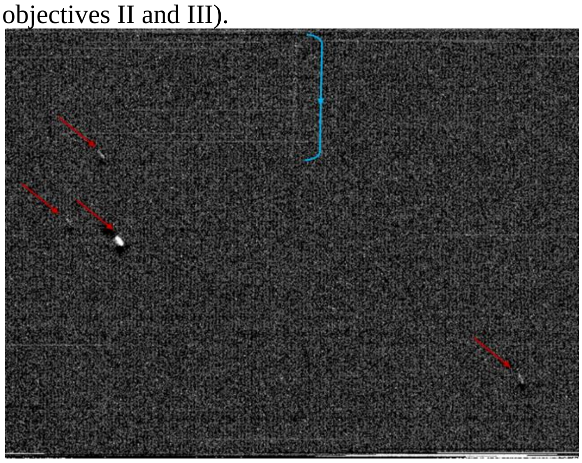

Figure 14: A targeted observation of a LEO object. The object is seen as a streak (blue marker). 4 stars are also visible (red arrows) as short streaks due to spacecraft attitude motion during image capture. The arrows indicate the stars' approximate direction of motion.

A number of attempts at imaging GEO objects have been conducted, but none have been successful. This is consistent with radiometric modelling of the VISCAM and GEO objects (see section 4.1).

7 Discussion and Conclusions

Given the nature of the spacecraft and services that Astroscale is operating and developing, ISSA is expected to be an important enabler and product of its missions. ISSA has the potential to provide a number of valuable improvements to SSA data availability, including improved accuracies/fidelities and access to new characterisation capabilities.

As a developer of IOS services, and by virtue of having spacecraft in orbit with sensors (optical and otherwise) needed for RPO, Astroscale is well placed to develop ISSA techniques – both by applying RPO sensors to SSA observations, and by using its spacecraft as platforms for dedicated SSA payloads.

The eight ISSA objectives outlined in section 3 demonstrate the wide variety of information and data types that ISSA can potentially provide. Addressing such a wide range of objectives will require a variety of sensing hardware, making use of dual-use RPO sensors but also relying on bespoke dedicated ISSA sensors. Indeed, it is clear from section 4 that small RPO cameras are physically limited in their ability to observe faint objects and address associated ISSA objectives (such as I and IV). Camera size can equally limit its utility for resolved imaging ISSA, but even low-resolution imagery – potentially captured from km distances – can provide vital information not available through ground-based SSA. The use of such an RPO camera in the ELSA-d imaging experiments (section 6) further demonstrates this. While the camera can capture LEO object streaks with well-defined geometry, a streak is yet to be captured with sufficient SNR to perform photometric characterisation. Under certain observations conditions, stray light and thermal noise are significant (sometimes leading to saturation). For ELSA-d's VISCAM, GEO objects are too faint to detect.

ISSA observations require high geometric and radiometric fidelities – higher than is often required for engineering sensors. Any sensors designed for conducting ISSA (whether they are dedicated sensors or also perform RPO functions) therefore require thorough pre-flight and in-flight calibration, as well as consideration and minimisation of noise sources in the hardware design (with the use of baffles, and consideration of detector temperature and cooling, for example).

ISSA is very much in the development, demonstration and maturation phase. Useful lessons are being learned from the ELSA-d imaging experiments. The ADRAS-J mission and the COSMIC mission study are valuable opportunities through which Astroscale is furthering its ISSA capabilities and developing novel ISSA hardware and analysis tools to support future IOS missions.

8 References

[1] ESA, "Space debris by the numbers," 2022. https://www.esa.int/Safety_Security/Space_Debris/Space_debris_by_the_numbers (accessed Mar. 03, 2022).

[2] J. A. Carroll, "A Clearer View of Orbital Debris," *1st Int'l. Orbital Debris Conf.*, 2019.

[3] D. Mehrholz, L. Leushacke, W. Flury, R. Jehn, H. Klinkrad, and M. Landgraf, "Detecting, Tracking and Imaging Space Debris," *ESA bulletin 109*, 2002.

[4] T. Schildknecht *et al.*, "PHOTOMETRIC MONITORING OF NON-RESOLVED SPACE DEBRIS AND DATA-BASES OF OPTICAL LIGHT CURVES," *2015 AMOS Technical Conf.*, pp. 15–18, 2015.

[5] J. Virtanen *et al.*, "Streak detection and analysis pipeline for space-debris optical images," *Advances in Space Research*, vol. 57, no. 8, pp. 1607–1623, Apr. 2016, doi: 10.1016/J.ASR.2015.09.024.

[6] J. R. Shell, "Optimizing orbital debris monitoring with optical telescopes," 2010.

[7] H. Krag *et al.*, "PROOF — The extension of esa's MASTER Model to predict debris detections," *Acta Astronaut*, vol. 47, no. 2–9, pp. 687–697, Jul. 2000, doi: 10.1016/S0094-5765(00)00106-5.

[8] V. I. Kudak, V. P. Epishev, V. M. Perig, and I. F. Neybauer, "Determining the orientation and spin period of TOPEX/Poseidon satellite by a photometric method," *Astrophysical Bulletin 2017 72:3*, vol. 72, pp. 340–348, 2017, doi: 10.1134/S1990341317030233.

[9] C. J. Wetterer and M. Jah, "Attitude Determination from Light Curves," *https://doi.org/10.2514/1.44254*, vol. 32, no. 5, pp. 1648–1651, 2012, doi: 10.2514/1.44254.

[10] A. Waszczak *et al.*, "ASTEROID LIGHT CURVES FROM THE PALOMAR TRANSIENT FACTORY SURVEY: ROTATION PERIODS AND PHASE FUNCTIONS FROM SPARSE PHOTOMETRY," *Astron J*, vol. 150, 2015, doi: 10.1088/0004-6256/150/3/75.

[11] S. Karpov *et al.*, "MASSIVE PHOTOMETRY OF LOW-ALTITUDE ARTIFICIAL SATELLITES ON MINI-MEGA-TORTORA," *RevMexAA*, vol. 48, pp. 112–113, 2016, Accessed: Aug. 19, 2022. [Online]. Available: http://www.space-track.org/

[12] T. Harris *et al.*, "Space Situational Awareness (SSA) activities explored through the ELSA-d mission," *AMOS 2021*, 2021, Accessed: Sep. 01, 2022. [Online]. Available: www.amostech.com

[13] E. J. Polidan *et al.*, "A study of hot pixel annealing in the Hubble Space Telescope Wide Field Camera 3 CCDs," *https://doi.org/10.1117/12.552111*, vol. 5487, pp. 289–298, Oct. 2004, doi: 10.1117/12.552111.